J Mol Model (2016) 22: 10
DOI 10.1007/s00894-015-2882-z

ORIGINAL PAPER

Theoretical study of the cooperative effects between the triel bond and the pnicogen bond in BF_3···$NCXH_2$···Y (X = P, As, Sb; Y = H_2O, NH_3) complexes

Ming-Xiu Liu[1] · **Hong-Ying Zhuo**[1] · **Qing-Zhong Li**[1] · **Wen-Zuo Li**[1] · **Jian-Bo Cheng**[1]

Received: 1 September 2015 / Accepted: 29 November 2015 / Published online: 16 December 2015

Abstract The interplay between the triel bond and the pnicogen bond in BF_3···$NCXH_2$···Y (X = P, As, Sb; Y = H_2O, NH_3) complexes was studied theoretically. Both bonds exhibited cooperative effects, with shorter binding distances, larger interaction energies, and greater electron densities found for the ternary complexes than for the corresponding binary ones. The cooperative effects between the triel bond and the pnicogen bond were probed by analyzing molecular electrostatic potentials, charge transfer, and orbital interactions. The results showed that the enhancement of the triel bond can mainly be attributed to the electrostatic interaction, while the strengthening of the pnicogen bond can be ascribed chiefly to the electrostatic and orbital interactions. In addition, the origins of both the triel bond and the pnicogen bond were deduced via energy decomposition.

Keywords Triel bonds · Pnicogen bonds · Synergistic effects

Introduction

Over the past few decades, the structural chemistry of Lewis acid–base complexes involving BF_3 has been the focus of many experimental and theoretical studies [1–12]. This interest stems partly from the fact that the dative linkages appear to be intermediate between van der Waals interactions and fully formed chemical bonds. Therefore, it has been demonstrated that these complexes can exhibit interesting structural chemistry and provide an unusual perspective on the evolution of molecular physical properties between the limits of van der Waals and chemical interactions [13]. Upon crystallization, these structures show dramatic changes in bond lengths and bond angles. For example, in the BF_3···NCH complex, the B–N distance and N–B–F angle are 1.638 Å and 105.6°, respectively, in the solid state [3], whereas the corresponding gas-phase values are 2.473 Å and 91.5°, as determined by microwave spectroscopy of a supersonic jet [4]. These structural changes are usually attributed to crystal packing effects, while a cooperative mechanism is responsible for the short B–N distance in the BF_3···NCH complex [14]. There have been lots of studies on the reactivity [15], thermodynamics [16], spectroscopy [17], and structures [18] of a wide range of Lewis acid–base complexes involving BF_3 since the concept of such complexes was first introduced by G.N. Lewis in 1923 [19]. Recently, Murray et al. [20] and Grabowski [21, 22] have labeled Lewis acid–base interactions involving BF_3 as π-hole interactions due to the presence of a π-hole (a region with positive electrostatic potential) on the boron atom. Clark and coauthors [23, 24] considered hydrogen bonding to be a σ-hole interaction and used this to explain the wide range of directionality of hydrogen bonding. Actually, researchers have tried to explain the formation of all intermolecular interaction types with the σ-hole concept, and it has been shown that many intermolecular interactions can indeed be explained as σ-hole interactions [23, 24]. It is now accepted that the existence of a σ-hole on an atom of a group IV–VII element is responsible for the formation of halogen [25–27], chalcogen [28–30], pnicogen [31–34], and tetrel [35–38] bonds.

Electronic supplementary material The online version of this article (doi:10.1007/s00894-015-2882-z) contains supplementary material, which is available to authorized users.

✉ Qing-Zhong Li
lqz@ytu.edu.cn

[1] The Laboratory of Theoretical and Computational Chemistry, School of Chemistry and Chemical Engineering, Yantai University, Yantai 264005, People's Republic of China

The pnicogen bond has recently been recognized as a new and important type of intermolecular interaction, based on the results of experimental [39–41] and theoretical [42–50] studies. In view of the role of the σ-hole in pnicogen bonding, the electrostatic interaction appears to be the main contributor to the stability of pnicogen-bonded complexes [49, 51]. As a result, the pnicogen bond becomes stronger with increasing pnicogen atomic mass [49, 51]. On the other hand, Scheiner thought that the stability of pnicogen-bonded complexes can be partly ascribed to charge transfer from the bonding orbital in a Lewis base to an antibonding orbital in the pnicogen donor [44]. Energy decomposition results also support this hypothesis for the origin of pnicogen bonds based on electrostatic potentials and orbital interactions. Although research into pnicogen bonding has only just started, the types of Lewis base that participate in it vary; they include lone pairs on F, N, and O atoms, π electrons in unsaturated hydrocarbons or aromatic compounds [51–53], σ electrons in metal hydrides [49, 54], and single electrons in radicals [55], anions [56], and carbenes [57]. The presence of so many studies of pnicogen bonds in the literature can be attributed to the fact that pnicogen bonding plays important roles in crystal materials [38, 52, 58], chemical reactions [55], and biological systems [59]. The above applications of pnicogen bonding are dependent on its directionality and strength. The introduction of substituents is an effective means of regulating the strength of a pnicogen bond. It has been demonstrated that pnicogen bond strength is reinforced by the presence of an electron-withdrawing substituent on the Lewis acid center and/or an electron-donating one on the Lewis base center [44, 60]. Another method of tuning the strength of a pnicogen bond is through cooperative effects generated by combining the pnicogen bond with other interactions [49, 60–67]. In the clusters $(PH_2F)_n$ and $(PH_2Cl)_n$, n=2–7, the pnicogen bonds strengthen as the length of the chain increases due to cooperative effects between the pnicogen bonds (caused mainly by the electrostatic interaction) [61]. The pnicogen bond in $(PH_2F)_2$ is also strengthened when an F–H···F hydrogen bond is introduced into this cluster [62]. The F–H···F hydrogen bond enhances the pnicogen bond in PH_2F–NH_2F when it forms at the P–F end, but it weakens the pnicogen bond when it occurs at the N–F end [63]. It has been shown that the pnicogen atom acts as a dual Lewis acid–base [66, 68]. Interestingly, however, in the complexes $H_3N\cdots FH_2X\cdots MCN$ (X = P, As; M = Cu, Ag, Au), where a pnicogen bond coexists with a coordination interaction, the stronger coordination interaction strengthens the weaker pnicogen bond while the pnicogen bond weakens the coordination interaction [68].

Cooperative effects are an important driving force for the formation of new chemical species, and play a critical role in accomplishing the functions associated with intermolecular interactions. In the work reported in the present paper, we studied the cooperative effects between the pnicogen bond and the triel bond in $BF_3\cdots NCXH_2\cdots H_2O$ and $BF_3\cdots NCXH_2\cdots NH_3$ (X = P, As, Sb) complexes, as shown in Fig. 1. The changes in the strengths of both of these bonds were estimated by analyzing binding distances, interaction energies, and electron densities. To unravel the mechanism for the cooperativity effects in these systems, natural bond orbital (NBO), molecular electrostatic potential, and energy decomposition investigations were performed for these complexes.

Theoretical methods

All calculations were performed using the Gaussian 09 program [69]. The structures of the complexes and the respective monomers were optimized using the second-order Møller–Plesset perturbation theory (MP2) with the aug-cc-pVTZ basis set for all atoms except antimony (Sb). The aug-cc-pVTZ-PP basis set, which uses small-core relativistic pseudopotentials to describe the inner core orbitals, was used for Sb to account for relativistic effects. Frequency calculations were carried out at the same level to confirm that the optimized structures were local minima on their potential surfaces. Interaction energies were computed with supermolecular methods in which the geometries of BF_3 were frozen in the complexes and those of other monomers were optimized. These quantities were corrected for basis set superposition error (BSSE) by the counterpoise procedure suggested by Boys and Bernardi [70].

Molecular electrostatic potentials (MEPs) on the 0.001-au electron density contour were calculated at the MP2/aug-cc-pVTZ level with the Wave Function Analysis–Surface Analysis Suite (WFA-SAS) program [71]. Topological analysis of all complexes was carried out using Bader's theory of

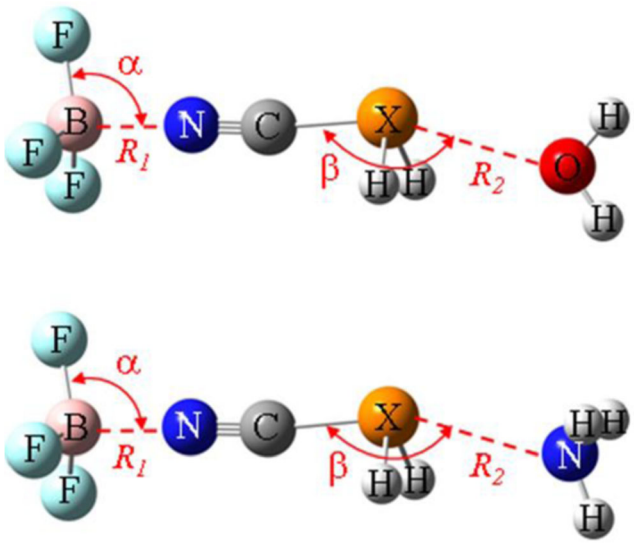

Fig. 1 Schema defining geometric parameters of the $BF_3\cdots NCXH_2\cdots H_2O$ and $BF_3\cdots NCXH_2\cdots NH_3$ (X = P, As, Sb) ternary systems

atoms in molecules (AIM) with the help of the AIM2000 software [72]. Natural bond orbital (NBO) analysis [73] was performed at the HF/aug-cc-pVTZ level via procedures included in Gaussian 09 in order to analyze orbital interactions and charge transfer. An energy decomposition analysis of the interaction energy was performed using the GAMESS program [74] with the localized molecular orbital–energy decomposition analysis (LMOEDA) method [75] at the MP2/aug-cc-pVTZ level.

Results and discussion

Pnicogen-bonded and triel-bonded dyads

Due to the electron-deficient nature of the boron atom, this atom is often considered a Lewis acid, i.e., it presents electron depletion (it has a π-hole) [76]. As a result, the boron atom in BF_3 forms a triel bond with the N atom of $NCXH_2$ (X = P, As, Sb). It is obvious from Fig. 1 that, upon the formation of the triel bond (i.e., with complexation), the planar BF_3 monomer becomes umbrella-structured; this phenomenon has also been observed in many Lewis acid–base complexes of BF_3 [1–12]. It has been shown that the structures of BF_3 complexes have structures that are between trigonal and tetrahedral [22]. This deformation is expected to be more prominent in the complexes with stronger triel bonds, as evidenced by a larger F–B···N angle (Table 1). As the atomic number of the pnicogen increases, the B···N distance shortens and the interaction energy becomes more negative, indicating that the triel bond strengthens. Grabowski stressed the importance of electrostatic interactions in triel bonds, based on the relationship between the electrostatic potential of the π-hole of the triel atom and the interaction energy [22]. Thus, we attempted to explain changes in the strength of triel bonding by linking them to changes in the negative electrostatic potential on the N atom of $NCXH_2$ (Table 2). It is clear that the electrostatic potential on the N atom of $NCXH_2$ becomes more negative when X is changed from P to Sb, due to the smaller electronegativity of the Sb atom. This is in line with the strength of triel bonding. The triel bond is stronger in BF_3···$NCXH_2$ than in BF_3···NCH, which has a binding distance of 2.364 Å and an interaction energy of −5.2 kcal/mol at the MP2/aug-cc-pVTZ level [22]. This shows that the group XH_2 is an electron donor when it is adjoined with the electron-withdrawing group CN.

The pnicogen bonds in the $NCXH_2$···H_2O and $NCXH_2$···NH_3 complexes are σ-hole interactions, unlike the triel bond in BF_3···$NCXH_2$. The strength of the pnicogen bond is dependent on the nature of atom X and the Lewis base. That is, the pnicogen bond is stronger (the binding distance is shorter and the interaction energy is larger) when X is heavier. This is consistent with the negative electrostatic potential on the X atom (Table 2). As expected, the presence of the stronger Lewis base NH_3 leads to a stronger pnicogen bond than the presence of the weaker Lewis base H_2O. Clearly, the pnicogen bonds in the $NCXH_2$···H_2O and $NCXH_2$···NH_3 complexes are much weaker than the triel bond in BF_3···$NCXH_2$. In addition, the pnicogen bond in $NCPH_2$···NH_3 is weaker than that in FPH_2···NH_3 [44], even though –CN is a stronger electron-withdrawing group. This means that other interactions besides the electrostatic interaction, such as charge transfer, are also important in the formation of pnicogen bonds [44]. A stronger pnicogen bond corresponds to a better oriented pnicogen bond, i.e., a bigger C–X···N/O angle.

The formation of the triel bond causes a different change in the C≡N bond length and a different shift in its frequency to those caused by the formation of the pnicogen bond. Specifically, the C≡N bond is shortened by the formation of the triel bond and the corresponding stretching vibration displays a blueshift, while the C≡N bond is elongated by the formation

Table 1 Equilibrium distances (R_1/R_2, Å), changes in the lengths of the C≡N and C–X bonds (Δr, Å), bond angles (α/β, degrees), shifts in the stretching frequency of the C≡N bond ($\Delta\nu$, cm^{-1}), and interaction energies (ΔE, kcal/mol) in the binary systems

Complex	R_1/R_2	$\Delta r_{C\equiv N}$	Δr_{C-X}	α/β	$\Delta\nu_{C\equiv N}$	ΔE
BF_3···$NCPH_2$	1.877	−0.009	0.005	100.2	75	−16.89
BF_3···$NCAsH_2$	1.829	−0.009	0.007	100.9	84	−19.14
BF_3···$NCSbH_2$	1.789	−0.010	0.016	101.5	90	−21.70
$NCPH_2$···H_2O	2.939	0.000	0.007	161.8	−3	−3.66
$NCAsH_2$···H_2O	2.907	0.001	0.012	160.5	−4	−3.94
$NCSbH_2$···H_2O	2.884	0.001	0.021	159.2	−3	−5.01
$NCPH_2$···NH_3	2.959	0.000	0.015	163.5	−7	−4.57
$NCAsH_2$···NH_3	2.908	0.001	0.024	161.8	−8	−5.13
$NCSbH_2$···NH_3	2.808	0.001	0.042	159.1	−8	−7.23

Table 2 The most positive molecular electrostatic potential (MEP) on the pnicogen atom (V_{max}, kcal/mol) in each triel-bonded binary complex and the most negative MEP on the N atom (V_{min}, kcal/mol) in each pnicogen-bonded binary complex, as well as those parameters in the corresponding monomers (in parentheses)

Complexes	V_{max}/V_{min}	ΔV
BF_3···$NCPH_2$	51.68 (36.61)	14.77
BF_3···$NCAsH_2$	54.63 (38.38)	16.25
BF_3···$NCSbH_2$	61.83 (44.38)	17.45
$NCPH_2$···H_2O	−39.45 (−34.56)	−4.89
$NCAsH_2$···H_2O	−40.88 (−35.53)	−5.35
$NCSbH_2$···H_2O	−42.99 (−36.90)	−6.09
$NCPH_2$···NH_3	−40.57 (−34.56)	−6.01
$NCAsH_2$···NH_3	−42.35 (−35.53)	−6.82
$NCSbH_2$···NH_3	−45.69 (−36.90)	−8.79

ΔV is the difference in MEP between the complex and the monomer

of the pnicogen bond and the respective stretching vibration shows a redshift. Moreover, the C≡N bond in the triel bond shows a larger change in bond length and a larger frequency shift than that in the pnicogen bond. The C–X bond is stretched whether it is in the triel bond or in the pnicogen bond.

The existence of the triel bond and the pnicogen bond is demonstrated by the presence of the B···N and X···O/N bond critical points (BCPs) in Fig. 2, respectively. Table 3 shows that the electron densities at these BCPs change in a manner consistent with the strength of the corresponding interaction. This supports a conclusion drawn based on numerous studies of hydrogen bonds—that the electron density at the intermolecular BCP often correlates with the strength of the interaction [77]. The electron density at the B···N BCP exceeds the range 0.002–0.04 au suggested for hydrogen bonds [78]; it corresponds to the (stronger) triel bond. The Laplacian of the electron density at the B···N BCP is positive for triel-bonded complexes, indicating that it cannot be classified as a covalent bond [79]. This also holds true for the pnicogen bonds. However, the energy densities at the B···N and Sb···N BCPs are negative, which is often attributed to a partially covalent interaction [79]. For the remaining interactions, the energy density is positive, corresponding to a pure closed-shell interaction [79].

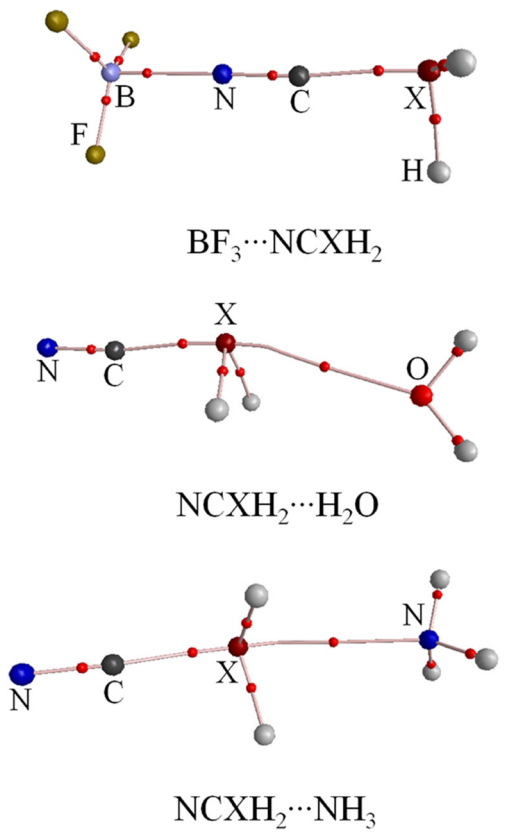

Fig. 2 Molecular maps of $BF_3\cdots NCXH_2$, $NCXH_2\cdots H_2O$, and $NCXH_2\cdots NH_3$ (X = P, As, Sb) along with bond critical points (*red points*)

Table 3 Electron density (ρ, au), Laplacian ($\nabla^2\rho$, au), and energy density (H, au) at the intermolecular bond critical point in the binary systems, as well as the second-order perturbation energy (E^2, kcal/mol) and charge transferred (CT, e) in those systems

Complexes	ρ	$\nabla^2\rho$	H	E^2	CT
$BF_3\cdots NCPH_2$	0.060	0.082	−0.036	–	0.163
$BF_3\cdots NCAsH_2$	0.067	0.154	−0.041	–	0.187
$BF_3\cdots NCSbH_2$	0.072	0.147	−0.047	–	0.206
$NCPH_2\cdots H_2O$	0.011	0.043	0.002	3.54	0.007
$NCAsH_2\cdots H_2O$	0.013	0.048	0.002	4.93	0.009
$NCSbH_2\cdots H_2O$	0.016	0.056	0.001	7.76	0.017
$NCPH_2\cdots NH_3$	0.015	0.042	0.001	6.56	0.018
$NCAsH_2\cdots NH_3$	0.018	0.048	0.001	9.33	0.025
$NCSbH_2\cdots NH_3$	0.026	0.056	−0.002	16.25	0.048

E^2 corresponds to the orbital interaction $LP_{N(O)} \rightarrow BD^*_{C-X}$, where $LP_{N(O)}$ is the lone pair on the N or O atom in the Lewis base and BD^*_{C-X} denotes the C–X antibonding orbital in $NCXH_2$ (X = P, As, Sb)

It was demonstrated that the two important orbital interactions $LP_N \rightarrow LP^*_B$ and $LP_N \rightarrow BD^*_{B-F}$ are present in the triel bond of the $BF_3\cdots NCH$ complex [22]. However, these orbital interactions are not found in $BF_3\cdots NCXH_2$ because the corresponding triel bond is classified as a covalent bond in the NBO approach. For the pnicogen bond, there is the orbital interaction $LP_{N(O)} \rightarrow BD^*_{C-X}$, where $LP_{N(O)}$ is the lone pair on the N or O atom in the Lewis base and BD^*_{C-X} denotes the C–X antibonding orbital in $NCXH_2$ (X = P, As, Sb). This orbital interaction correlates with the interaction energy of the pnicogen bond, indicating that the orbital interaction is also important for the formation of the pnicogen bond. This orbital interaction is also responsible for the elongation of the C–X bond in the pnicogen bond. It is clear that charge transfer occurs from the Lewis base to the Lewis acid upon complexation. The formation of the triel bond is associated with considerable charge transfer, 0.16~0.21e, consistent with the nature of a covalent interaction. Clearly, the charge transfer in $BF_3\cdots NCXH_2$ is much larger than that (0.034e) in $BF_3\cdots NCH$ [20]. Less charge is transferred upon the formation of the pnicogen bond, but the charge transfer is again correlated with the interaction strength.

To elucidate the origins of the triel bond and the pnicogen bond, the energies of both interactions were decomposed into five components: electrostatic energy (E^{ele}), exchange energy (E^{ex}), repulsion energy (E^{rep}), polarization energy (E^{pol}), and dispersion energy (E^{disp}). Table 4 shows that the triel bond has a larger exchange energy, which corresponds to a bigger overlap between the molecular orbitals of both molecules, although it also has a larger repulsion energy due to the shorter distance between molecules. For the triel bond, the electrostatic energy is comparable with the polarization energy. The relatively large polarization energy suggests that the shapes

Table 4 Values for the electrostatic energy (E^{ele}), exchange energy (E^{ex}), repulsion energy (E^{rep}), polarization energy (E^{pol}), dispersion energy (E^{disp}), and interaction energy (E^{int}) in the binary systems. All values are in kcal/mol

Complex	E^{ele}	E^{ex}	E^{rep}	E^{pol}	E^{disp}	E^{int}
$BF_3\cdots NCPH_2$	−39.57	−54.88	110.52	−30.43	−2.64	−17.01
$BF_3\cdots NCAsH_2$	−44.37	−61.59	124.94	−35.89	−2.41	−19.32
$BF_3\cdots NCSbH_2$	−49.21	−67.94	138.66	−41.38	−2.09	−21.96
$NCPH_2\cdots H_2O$	−5.74	−6.47	11.05	−1.37	−1.20	−3.72
$NCAsH_2\cdots H_2O$	−7.02	−8.36	14.47	−1.81	−1.31	−4.03
$NCSbH_2\cdots H_2O$	−10.18	−12.72	22.34	−3.21	−1.38	−5.15
$NCPH_2\cdots NH_3$	−9.05	−12.73	21.83	−2.77	−1.99	−4.73
$NCAsH_2\cdots NH_3$	−12.00	−16.87	29.53	−3.80	−2.24	−5.38
$NCSbH_2\cdots NH_3$	−19.76	−28.90	51.63	−8.03	−2.67	−7.72

of the orbitals change significantly, which is a typical characteristic of the formation of a covalent bond. For the pnicogen bond, the electrostatic interaction is dominant since the electrostatic energy is more negative than the polarization and dispersion energies. Very recently, Politzer and coauthors pointed out that the Hellmann–Feynman theorem can provide a straightforward interpretation of hydrogen-bond and other σ-hole interactions in terms of Coulombic interactions, which encompasses polarization and therefore dispersion [80].

Interplay between the pnicogen bond and the triel bond

The geometric and energetic results computed for the ternary complexes are summarized in Tables 5 and 6, respectively. For the triel and pnicogen bonds, the binding distance is shorter and the interaction energy more negative for the ternary complexes than for the respective binary systems. This indicates that both the triel bond and the pnicogen bond are stronger in the ternary systems than in the binary systems. This conclusion is further supported by the increases in electron density at the B···N and X···O/N BCPs in the ternary complexes as compared to the binary complexes (Table S1 in the "Electronic supplementary material," ESM). The shortening of the B···N distance varies from 0.057 Å in $BF_3\cdots NCSbH_2\cdots H_2O$ to 0.116 Å in $BF_3\cdots NCPH_2\cdots NH_3$; the shortening of the B···N distance is thus clearly related to the strength of the pnicogen bond. For a given Lewis base in the pnicogen bond, the B···N distance shortens less as the pnicogen bond interaction strength increases. However, for the same pnicogen atom, the B···N shortens more when the stronger Lewis base (NH_3) is used. The shortening of the X···O/N distance ranges from 0.120 to 0.187 Å, which is larger than the shortening of the B···N distance. This result contrasts with that seen for $BF_3\cdots NCH\cdots NCH$ [81]; in this case, the B···N distance shortens much more than the H···N distance does. Obviously, the dependence of the shortening of the X···O distance on the strength of the triel bond is the reverse of the dependence of the shortening of the X···N distance on the strength of the triel bond. That is, enhancing the strength of the triel bond leads to greater shortening of the X···O distance but less shortening of the X···N distance. When both the triel bond and the pnicogen bond are strengthened, the F–B···N angle increases a little while the C–X···O/N angle changes only slightly.

The increase in the bond interaction energy as a percentage of the total interaction energy is more prominent for the pnicogen bonds than for the triel bonds. The strengthening of both the triel bond and the pnicogen bond in each ternary complex indicates that these interactions show a synergistic effect. The presence of this synergistic effect is further confirmed by the negative cooperative energy (E_{coop}). The cooperative energy makes the largest contribution to the stability of each ternary complex (17.1–25.6 % of the total interaction energy). This contribution is larger than that of the cooperativity between the hydrogen bond and the pnicogen bond [50, 60]. E_{coop} as a percentage of the total interaction energy correlates with the strength of the triel bond and that of the pnicogen bond. In particular, it increases when the Lewis base is changed from H_2O to NH_3 but decreases when it is changed from P to Sb. As a result, the largest contribution is obtained for the cooperative energy in $BF_3\cdots NCPH_2\cdots NH_3$.

The C≡N bond is contracted in each ternary complex (Table S2 in the ESM), and this contraction is larger than that in the corresponding binary system, while the C–X bond is elongated and its elongation is greater than that in the corresponding binary system due to the interplay between the triel bond and the pnicogen bond. The C≡N stretching vibration thus exhibits a blueshift for each ternary complex. The blueshifts for the ternary complexes of H_2O are larger than those

Table 5 Equilibrium distances (R, Å) and bond angles (α/β, degrees) in the ternary systems, as well as the changes in these parameters (in parentheses) relative to those of the corresponding binary systems

Complex	R_1	R_2	α	β
$BF_3\cdots NCPH_2\cdots H_2O$	1.785 (−0.092)	2.819 (−0.120)	101.8 (1.6)	161.4 (−0.4)
$BF_3\cdots NCAsH_2\cdots H_2O$	1.762 (−0.067)	2.787 (−0.120)	102.2 (1.3)	160.5 (0.0)
$BF_3\cdots NCSbH_2\cdots H_2O$	1.732 (−0.057)	2.742 (−0.142)	102.7 (1.2)	159.3 (0.1)
$BF_3\cdots NCPH_2\cdots NH_3$	1.761 (−0.116)	2.772 (−0.187)	102.1 (1.9)	164.0 (0.5)
$BF_3\cdots NCAsH_2\cdots NH_3$	1.739 (−0.090)	2.724 (−0.184)	102.7 (1.8)	162.1 (0.3)
$BF_3\cdots NCSbH_2\cdots NH_3$	1.708 (−0.081)	2.636 (−0.172)	103.3 (1.8)	158.7 (−0.4)

Table 6 Total interaction energy (ΔE_{total}) of each ternary system, the interaction energies (ΔE) of the triel bond (TB) and the pnicogen bond (ZB) in each ternary system as well as the changes in these energies ($\Delta\Delta E$) relative to those of the binary systems, and the cooperative energy (E_{coop}) of each ternary system. All values are in kcal/mol

Complexes	ΔE_{total}	ΔE_{TB}	$\Delta\Delta E_{TB}$	ΔE_{ZB}	$\Delta\Delta E_{ZB}$	E_{coop}
$BF_3\cdots NCPH_2\cdots H_2O$	−26.35	−22.47	−5.58	−5.20	−1.54	−5.54 (21.0)
$BF_3\cdots NCAsH_2\cdots H_2O$	−28.46	−24.40	−5.26	−5.67	−1.73	−5.13 (18.0)
$BF_3\cdots NCSbH_2\cdots H_2O$	−32.54	−27.49	−5.79	−7.25	−2.24	−5.57 (17.1)
$BF_3\cdots NCPH_2\cdots NH_3$	−29.25	−24.45	−7.56	−6.78	−2.21	−7.49 (25.6)
$BF_3\cdots NCAsH_2\cdots NH_3$	−31.95	−26.75	−7.61	−7.72	−2.59	−7.37 (23.1)
$BF_3\cdots NCSbH_2\cdots NH_3$	−37.88	−30.84	−9.14	−10.80	−3.57	−8.65 (22.8)

Data in parentheses are E_{coop} as percentages of the total interaction energy. E_{coop} was calculated via $E_{coop} = \Delta E_{total} - \Delta E_{TB}(D) - \Delta E_{ZB}(D) - \Delta E_{far}$, in which $\Delta E_{TB}(D)$ and $\Delta E_{ZB}(D)$ are the interaction energies of the optimized dimers $BF_3\cdots NCXH_2$ and $NCXH_2\cdots H_2O/NH_3$, respectively, while ΔE_{far} is the interaction energy between BF_3 and H_2O/NH_3, with their geometries frozen in the ternary complexes

for the corresponding $BF_3\cdots NCXH_2$ complexes but smaller than those for the ternary complexes of NH_3.

When $NCXH_2$ forms a pnicogen bond with H_2O or NH_3, the negative MEP on the N atom of $NCXH_2$ is larger than that on the N atom of the $NCXH_2$ monomer (Table 2). This shows that the N atom of $NCXH_2$ in the $NCXH_2\cdots H_2O$ and $NCXH_2\cdots NH_3$ complexes is a stronger Lewis base when there is a triel bond, so the electrostatic interaction enhances the triel bond in each ternary complex. When $NCXH_2$ forms a triel bond with BF_3, the positive MEP on the X atom of $NCXH_2$ is larger than that on the X atom of the $NCXH_2$ monomer (Table 2). Furthermore, the increase in the positive MEP on the X atom of $NCXH_2$ shows a consistent change as the pnicogen bond is strengthened. This indicates that the enhancement of the pnicogen bond can mainly be attributed to the electrostatic interaction.

Table 7 presents the charge transferred in the triel bond and the pnicogen bond as well as the second-order perturbation energy of the pnicogen bond in each ternary complex. It is clear that more charge is transferred in both interactions in the ternary complexes as compared to the corresponding binary complexes. However, this increase in the charge transferred shows a consistent change with increasing interaction energy of the pnicogen bond, but not with increasing interaction energy of the triel bond. The $LP_{N(O)} \rightarrow BD^*_{C-X}$ orbital interaction is stronger in the ternary complexes, and the increase in the associated perturbation energy shows a consistent change with increasing pnicogen bond interaction energy. This means that this orbital interaction also enhances the pnicogen bond.

Table 7 Charge transferred (CT, e) in the triel bond (TB) and the pnicogen bond (ZB) of each ternary system as well as the difference in charge transferred (Δ) with respect to the corresponding binary systems; the second-order perturbation energy (E^2, kcal/mol) in each ternary system is also shown

Complex	CT_{TB}	ΔCT_{TB}	CT_{ZB}	ΔCT_{ZB}	E^2	ΔE^2
$BF_3\cdots NCPH_2\cdots H_2O$	0.212	0.049	0.012	0.005	5.38	1.84
$BF_3\cdots NCAsH_2\cdots H_2O$	0.224	0.037	0.015	0.006	7.35	2.42
$BF_3\cdots NCSbH_2\cdots H_2O$	0.242	0.036	0.026	0.009	12.28	4.52
$BF_3\cdots NCPH_2\cdots NH_3$	0.224	0.061	0.035	0.017	11.67	5.11
$BF_3\cdots NCAsH_2\cdots NH_3$	0.238	0.051	0.047	0.022	16.86	7.53
$BF_3\cdots NCSbH_2\cdots NH_3$	0.259	0.052	0.078	0.030	26.61	10.36

Conclusions

Ab initio calculations have been performed for the ternary complexes $BF_3\cdots NCXH_2\cdots Y$ (X = P, As, Sb; Y = H_2O, NH_3) and their respective binary complexes. The triel bond in $BF_3\cdots NCXH_2$ is partially covalent and becomes stronger when X is changed from P to Sb. The pnicogen bond in $NCXH_2\cdots Y$ is governed by the electrostatic interaction and becomes stronger as the X atom becomes heavier and the Lewis base Y becomes stronger. When the triel bond and pnicogen bond coexist in the same ternary complex, both interactions are strengthened by considerable cooperative energy. The pnicogen bond is enhanced more than the triel bond. The strengthening of both the triel bond and the pnicogen bond can be explained by the more negative electrostatic potential on the N atom in $NCXH_2\cdots Y$ and the more positive electrostatic potential on the X atom in $BF_3\cdots NCXH_2$, respectively.

Acknowledgments This work was supported by the National Natural Science Foundation of China (21573188).

References

1. Jurgens R, Almlöf J (1991) Chem Phys Lett 176:263–265
2. Dvorak MA, Ford RS, Suenram RD, Lovas FJ, Leopold KR (1992) J Am Chem Soc 114:108–114
3. Burns WA, Leopold KR (1993) J Am Chem Soc 115:11622–11623
4. Reeve SW, Burns WA, Lovas FJ, Suenram RD, Leopold KR (1993) J Phys Chem 97:10630–10637
5. Jiao HJ, Schleyer PR (1994) J Am Chem Soc 116:7429–7430
6. Fujiang D, Fowler PW, Legon AC (1995) J Chem Soc Chem Commun 24:113–114
7. Leopold KR, Canagaratna M, Phillips JA (1997) Acc Chem Res 30: 57–64

8. Wells NP, Phillips JA (2002) J Phys Chem A 106:1518–1523
9. Giesen DJ, Phillips JA (2003) J Phys Chem A 107:4009–4018
10. Venter G, Dillen J (2004) J Phys Chem A 108:8378–8384
11. Phillips JA, Giesen DJ, Wells NP, Halfen JA, Knutson CC, Wrass JP (2005) J Phys Chem A 109:8199–8208
12. Hase Y (2007) Spectrochim Acta A 68:734–738
13. Hunt SW, Leopold KR (2001) J Phys Chem A 105:5498–5506
14. Cabaleiro-Lago EM, Rios MA (1998) Chem Phys Lett 294:272–276
15. Jensen WB (1980) The Lewis acid–base concepts: an overview. Wiley-Interscience, New York
16. Pearson RG (1997) Chemical hardness—applications from molecules to solids. Wiley, Weinheim
17. Mulliken RS, Person WB (1969) Molecular complexes. Wiley, New York
18. Hargittai M, Hargittai I (1977) The molecular geometries of coordination compounds in the vapor phase. Elsevier, Amsterdam
19. Lewis GN (1923) Valence and the structure of atoms and molecules. The Chemical Catalog Company, Inc., New York
20. Murray JS, Lane P, Clark T, Riley KE, Politzer P (2012) J Mol Model 18:541–548
21. Grabowski SJ (2015) ChemPhysChem 16:1470–1479
22. Grabowski SJ (2014) ChemPhysChem 15:2985–2993
23. Hennemann M, Murray JS, Politzer P, Riley KE, Clark T (2012) J Mol Model 18:2461–2469
24. Politzer P, Murray JS, Clark T (2013) Phys Chem Chem Phys 15: 11178–11189
25. Metrangolo P, Neukirch H, Pilati T, Resnati G (2005) Acc Chem Res 38:386–395
26. Metrangolo P, Meyer F, Pilati T, Proserpio DM, Resnati G (2007) Chem Eur J 13:5765–5772
27. Cavallo G, Metrangolo P, Pilati T, Resnati G, Sansotera M, Terraneo G (2010) Chem Soc Rev 3:3772–3783
28. Sanz P, Mó O, Yanez M (2002) J Phys Chem A 106:4661–4668
29. Wang W, Ji B, Zhang Y (2009) J Phys Chem A 113:8132–8135
30. Murray JS, Lane P, Clark T, Politzer P (2007) J Mol Model 13: 1033–1038
31. Del Bene JE, Alkorta I, Sanchez-Sanz G, Elguero J (2011) J Phys Chem A 115:13724–13731
32. Scheiner S (2011) Chem Phys Lett 514:32–35
33. Grabowski SJ (2013) Chem Eur J 19:14600–14611
34. Murray JS, Lane P, Politzer P (2007) Int J Quantum Chem 107: 2286–2292
35. Grabowski SJ (2014) Phys Chem Chem Phys 16:1824–1834
36. Mani D, Arunan E (2013) Phys Chem Chem Phys 15:14377–14383
37. Bauz A, Mooibroek TJ, Frontera A (2013) Angew Chem Int Ed 52: 12317–12321
38. Murray JS, Lane P, Politzer P (2009) J Mol Model 15:723–729
39. Zahn S, Frank R, Hey-Hawkins E, Kirchner B (2011) Chem Eur J 17:6034–6038
40. Joshi PR, Ramanathan N, Sundararajan K, Sankaran K (2015) J Phys Chem A 119:3440–3451
41. Sarkar S, Pavan MS, Row TNG (2015) Phys Chem Chem Phys 17: 2330–2334
42. Solimannejad M, Gharabaghi M, Scheiner S (2011) J Chem Phys 134:024312
43. Scheiner S (2011) J Chem Phys 134:094315
44. Scheiner S (2011) J Phys Chem A 115:11202–11209
45. Adhikari U, Scheiner S (2012) J Phys Chem A 116:3487–3497
46. Adhikari U, Scheiner S (2012) Chem Phys Lett 532:31–35
47. Scheiner S (2011) J Chem Phys 134:164313
48. Scheiner S, Adhikari U (2011) J Phys Chem A 115:11101–11110
49. Li QZ, Li R, Liu XF, Li WZ, Cheng JB (2012) J Phys Chem A 116: 2547–2553
50. Li QZ, Li R, Liu XF, Li WZ, Cheng JB (2012) ChemPhysChem 13: 1205–1212
51. An XL, Li R, Li QZ, Liu XF, Li WZ, Cheng JB (2012) J Mol Model 18:4325–4332
52. Bauzá A, Quiñonero D, Deyá PM, Frontera A (2013) CrystEngComm 15:3137–3144
53. Xu HY, Wang W, Zou JW (2013) Acta Chim Sin 71:1175–1182
54. Ma FY, Li AY (2014) Comput Theor Chem 1045:78–85
55. Alkorta I, Elguero J, Solimannejad M (2014) J Phys Chem A 118: 947–953
56. Del Bene JE, Alkorta I, Elguero J (2014) J Phys Chem A 118:3386–3392
57. Zhuo HY, Li QZ (2015) Phys Chem Chem Phys 17:9153–9160
58. Politzer P, Murray JS, Janjić GV, Zarić SD (2014) Crystals 4:12–31
59. Bauzá A, Quiñonero D, Deyá PM, Frontera A (2012) Phys Chem Chem Phys 14:14061–14066
60. Del Bene JE, Alkorta I, Elguero J (2014) J Phys Chem A 118:2360–2366
61. Esrafili MD, Vakili M, Solimannejad M (2014) Chem Phys Lett 609:37–41
62. Alkorta I, Sánchez-Sanz G, Elguero J, Del Bene JE (2012) J Chem Theory Comput 8:2320–2327
63. Del Bene JE, Alkorta I, Sánchez-Sanz G, Elguero J (2012) J Phys Chem A 116:9205–9213
64. Esrafilia MD, Mohammadian-Sabeta F, Solimannejad M (2015) J Mol Graph Model 57:99–105
65. Solimannejad M, Ramezani V, Trujillo C, Alkorta I, Sánchez-Sanz G, Elguero J (2012) J Phys Chem A 116:5199–5206
66. Del Bene JE, Alkorta I, Sánchez-Sanz G, Elguero J (2013) J Phys Chem A 117:3133–3141
67. Zhuo HY, Li QZ, Li WZ, Cheng JB (2014) J Chem Phys 141: 244305
68. Zhuo HY, Li QZ, Li WZ, Cheng JB (2015) New J Chem 39:2067–2074
69. Frisch MJ, Trucks GW, Schlegel HB, Scuseria GE, Robb MA, Cheeseman JR, Montgomery JA Jr, Vreven T, Kudin KN, Burant JC, Millam JM, Iyengar SS, Tomasi J, Barone V, Mennucci B, Scalmani G, Cossi M, Rega N, Petersson GA, Nakatsuji H, Hada M, Ehara M, Toyota K, Fukuda R, Hasegawa J, Ishida M, Nakajima T, Honda Y, Kitao O, Nakai H, KleneMLX KJE, Hratchian HP, Cross JB, Adamo C, Jaramillo J, Gomperts R, Stratmann RE, Yazyev O, Austin AJ, Cammi R, Pomelli C, Ochterski JW, Ayala PY, Morokuma K, Voth GA, Salvador P, Dannenberg JJ, ZakrzewskiVG DS, Daniels AD, Strain MC, Farkas O, Malick DK, Rabuck AD, Raghavachari K, Foresman JB, Ortiz JV, Cui Q, Baboul AG, Clifford S, Cioslowski J, Stefanov BB, Liu G, Liashenko A, Piskorz P, Komaromi I, Martin RL, Fox DJ, Keith T, Al-LahamMA PCY, Nanayakkara A, Challacombe M, Gill PMW, Johnson B, Chen W, Gonzalez C, Wong MW, Pittsburgh PA, Pople JA (2009) Gaussian 09, revision A02. Gaussian Inc., Wallingford
70. Boys SF, Bernardi F (1970) Mol Phys 19:553–566
71. Bulat FA, Toro-Labbé A, Brinck T, Murray JS, Politzer P (2010) J Mol Model 16:1679–1691
72. Bader RFW (2000) AIM2000 program, version 2.0. McMaster University, Hamilton
73. Reed AE, Curtiss LA, Weinhold FA (1988) Chem Rev 88:899–926
74. Schmidt MW, Baldridge KK, Boalz JA, Elbert ST, Gorden MS, Jensen JH, Koseki S, Matsunaga N, Nguyen KA, Su SJ, Windus TL, Dupuis M, Montgomery JA (1993) J Comput Chem 14:1347–1363
75. Su PF, Li H (2009) J Chem Phys 13:014102
76. Politzer P, Murray JS, Clark T (2010) Phys Chem Chem Phys 12: 7748–7757
77. Parthasarathi R, Subramanian V, Sathyamurthy N (2006) J Phys Chem A 110:3349–3351
78. Koch U, Popelier PLA (1995) J Phys Chem A 99:9747–9754
79. Arnold WD, Oldfield E (2000) J Am Chem Soc 122:12835–12841
80. Politzer P, Murray JS, Clark T (2015) J Mol Model 21:52
81. Fiacco DL, Leopold KR (2003) J Phys Chem A 107:2808–2814